UAV Multi-Sensor Payloads for High Precision Aerial Surveys

Mohamed MOSTAFA, Srdjan SOBOL, and Joe HUTTON, Canada

Key words: UAV, unmanned, camera, GNSS, inertial, photogrammetry, LiDAR

SUMMARY

The Surveying industry has been evolving by implementing drones in their daily surveying and mapping activities over the last decade. Some UAV payloads, however, necessitate the presence of numerous ground control points (GCPs) which almost defeats the purpose of surveying the land from the air.

This paper presents the integration of professional-grade aerial survey sensors including GNSS, IMU, cameras, and LiDAR for high precision aerial surveys without the need for ground control points. The integration of these sensors as a drone payload allows for precisely surveying any topography to produce a variety of 2D and 3D mapping products including orthomosaics, digital surface models (DSM), colorized point clouds, topographic maps, etc. For a successful integration of a multi-sensor system as a drone payload, several integration parameters need to properly be addressed including individual sensor calibration (such as camera calibration) as well as spatial offsets (e.g., lever arms) and orientation misalignments (boresight), etc. Camera and/or LiDAR boresight calibration requires a certain flight pattern, processing mechanism, etc. This paper presents the best practice for system calibration.

To conduct a successful drone surveying mission, proper project planning, flight planning, data acquisition, data processing, and quality control are all needed to end up with a successful, accurate, and consistent mapping product. Therefore, this paper will address the best practices for the entire recipe of high precision aerial survey by drones. Additionally, the results of multiple geometric accuracy assessment projects using different drones, cameras, and LiDARs are presented.

1. INTRODUCTION

The development of low cost, easy to fly UAV's has enabled a new type of surveying capability using GNSS. Mounting GNSS on a UAV enables the receiver to be lifted above the ground to a vantage point above where obstructions can cause signal interruption and multipath. Adding a camera and LiDAR with an Inertial Measurement Unit (IMU) to compute orientation enables the precise high density ground coordinates of each pixel and point to be computed over a broad area limited only by the field of view of the imaging sensors and the trajectory of the UAV. This results in an enormous productivity improvement over the traditional surveying method of collecting discrete GNSS points from the ground.

The accuracy of the ground coordinates starts with the accuracy of the GNSS position measurements at the Antenna Phase Center (APC) located on the UAV. This accuracy is translated to ground through the knowledge of the fixed relative position of the GNSS antenna with respect to the camera and LiDAR sensors (GNSS Lever Arms), measurement of the orientation of the sensors with respect to the ground computed from the IMU, and direct range measurements from the LiDAR (or in the case of a camera only image scale determined from stereo images or from a pre-existing Digital Elevation Model). The final accuracy of the ground coordinates is hence a summation of the GNSS position error with error in the lever arms, errors in the orientation including boresight errors of the IMU with respect to the sensors, and errors in the sensor range measurements themselves.

Many UAV payloads with camera only or even camera with LiDAR attempt to minimize the ground error using numerous Ground Control Points (GCP) and classical aerial triangulation methods, which greatly reduces the efficiency of using a UAV to do surveying and increases the cost. This paper shows that a professionally integrated payload with proper calibration, the right software tools, and best operational practices can produce ground coordinate accuracies at the cm level without the need for dense GCP's.

2. DIRECT GEOREFERENCING

The technique for assigning coordinates to the pixels and points from a camera and LiDAR payload on a UAV using a GNSS and IMU is called Direct Georeferencing (DG). DG is a well established method for mapping and surveying from mobile platforms such as crewed aircraft (c.f., Mostafa and Schwarz, 2001), land vehicles and marine vessels (c.f., Li et al, 2004). With the introduction of UAV's for surveying, purpose built DG solutions for these platforms have been developed and integrated with a number of different sensors (Colomina and Molina, 2014; Mian et al, 2016; Mostafa, 2017; Hutton et al, 2020). The Trimble APX-15 UAV is an example of such a system (shown in Figure 1).

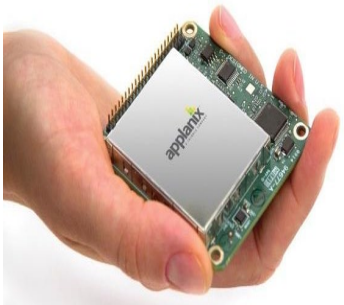

Figure 1: Trimble APX-15 UAV

It consists of a survey grade GNSS receiver and a high performance IMU integrated onto a small, low power, light weight board ideal for integration with UAV payloads. It also includes the POSPac UAV post-processing SW that provides key functionalities:

- Generation of centimeter accuracy combined forward and reverse GNSS-Aided Inertial position and orientation of the sensor (trajectory) using GNSS augmentation data
- Calibration of IMU to camera and IMU to LiDAR boresight angles (CalQC and LiDAR QC Modules)
- Calibration of Camera interior orientation (CalQC Module)
- Computation of Exterior Orientation for each image and LiDAR range in local mapping frame and datum.
- Optional adjustment of the trajectory using the LiDAR point cloud (LiDAR QC module)

The DG solution (Real-time and in post-processing) automatically computes the position and orientation of the sensor origin (LiDAR and Camera) as follows:

$$p_c^M = p_G^M - R_s^M(l_{c-G}^s + l_{c-b}^s)$$
$$R_s^M = R_b^M\, R_s^b \qquad (1)$$

where:
p_c^M = position of sensor origin in mapping frame,
p_G^M = position of GNSS APC in mapping frame,
R_s^M= rotation matrix from sensor frame to mapping frame
R_b^M= rotation matrix from IMU frame to mapping frame computed by onboard IMU,
R_s^b= rotation matrix from sensor frame to IMU frame (boresight),
l_{c-G}^s = lever arm from sensor origin to the GNSS APC in sensor frame,
l_{c-b}^s = lever arm from sensor origin to the IMU origin in sensor frame

The position of the sensor origin and the rotation matrix R_s^M are then used to compute the ground coordinates of the camera pixels and LiDAR points as follows:

$$p_i^M = p_c^M + R_s^M r_i^s \qquad (2)$$

where:
p_i^M = position of pixel or point *i* in the mapping frame,
r_i^s = LiDAR range *i* from sensor origin to the ground in the LiDAR frame ***or***
$r_i^s = S_i\ r_i^s$ with S_i = image Scale, r_i^s = vector from camera origin to pixel *i* in image frame

The lever arms and boresight are installation parameters of the DG system that need to be calibrated to a high level of accuracy so they do not contribute significantly to the positioning error on the ground. Other required calibration parameters include sensor specific parameters such as the camera interior orientation (principle point, lens distortions, focal length).

3. PAYLOAD INTEGRATION

A professional UAV payload for surveying and mapping integrates the DG system with the imaging sensors using the following best practices summarized in the following sections.

3.1 IMU Mounting

Since the IMU needs to measure the exact orientation of the sensor at a very high rate (at least 100 to 200 times a second) it must be rigidly attached to the sensor so that:

- There is no relative motion between the IMU and sensor under high dynamics or vibration. If the sensor moves even slightly with respect to the IMU, then this motion cannot be measured by the IMU and hence shows up as an extra error in the measured position and orientation (primarily the orientation)

- There is no long term relative motion of the IMU with respect to the sensor caused by aging or temperature effects. This will show up as a changing IMU boresight error.

3.2 IMU Boresight Measurement

The orientation measured by the DG system is the roll, pitch and heading from North computed by the accelerometer and gyro data output by the IMU about its body reference frame. The IMU body frame is defined by the internal accelerometer triad, and only has a nominal physical relationship to the IMU housing. So even if the IMU is physically mounted to be aligned with the imaging sensor frame, there are still small angular misalignments of the IMU body frame with respect to the sensor frame that need to be accounted for. If these misalignment angles are not corrected, they appear as additional errors in the measurement of the sensor orientation. The process of measuring the IMU misalignment with respect to the sensor frame is called boresighting the IMU to the sensor (and hence why they are called boresight angles). The accuracy of the boresight measurement must be below the orientation accuracy of the DG system to ensure there is no significant reduction of the accuracy in georeferencing the points and pixels on the ground.

The most practical and accurate method of boresighting an IMU to a sensor is to use an insitu process flying the payload in a so-called boresight flight. This procedure involves flying the payload with a specific trajectory with opposing and cross flight lines (as shown in Figure 2) such that the imagery and LiDAR scans overlap each other in such a way that the boresight angles can be measured by determining how the computed ground coordinates of the pixels and points are shifted relative to each other. It is important to note that the boresight measurement does not require Ground Control Points.

3.3 Sensor to IMU Lever Arm Measurement

Like the orientation, the DG system will automatically compute the position from the IMU data at the origin of the IMU (the intersection of the triads of the accelerometers). Hence in order to produce measurements of the sensor origin, the position must be translated from the IMU origin to the sensor origin. This is done by precisely measuring the vector offset from the sensor origin to the IMU origin, the accuracy of which must be well below what can be achieved by the GNSS so the overall georeferencing accuracy is not reduced.

The IMU and sensor origins are well calibrated and provided by the manufacturers, which enables the lever arm vector to be determined to mm accuracy, well below the GNSS error floor of a few cm.

3.4 Electrical Integration

Since the GNSS receiver is using radio signal phase Measurements to determine position, a proper electrical integration of the DG system is required. This means proper shielding must be used to avoid Radio Frequency Interference from external sources such as motors and even the LiDAR itself. Too much RFI will reduce the SNR of the GNSS signals, preventing the DG system from obtaining a high accuracy position at the cm level.

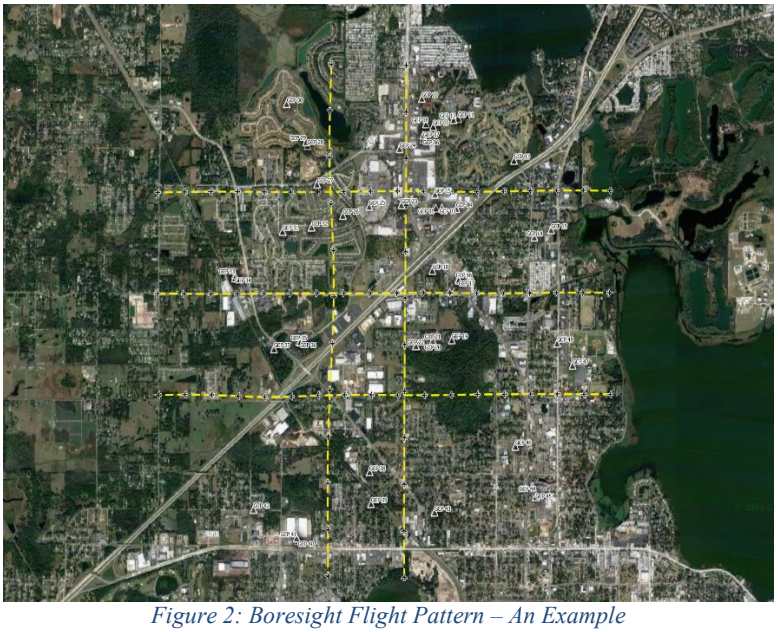

Figure 2: Boresight Flight Pattern – An Example

Figure 3: GeoCue TruView Camera + LiDAR

Figure 4: PhaseOne 100MP Camera

3.5 Payload Vibration Isolation

All IMU's have a finite bandwidth over which they can measure motion. Hence in order to obtain the highest level of accuracy it is critical that the entire payload (sensor integrated with IMU) must be mounted to the UAV with proper vibration isolators to filter out vibrations from the motors. This not only prevents erroneous measurements from the DG system, it also protects the imaging sensors and improves the quality of the data they collect.

3.6 GNSS Antenna Placement

Equally important to the collection of quality GNSS observables is the placement of the GNSS antenna. It must be located high enough above the airframe to avoid shading by propellers or wings with the UAV turns, and to avoid RFI noise from the motors being transmitted into the antenna.

3.7 Sensor to GNSS APC Lever Arm Measurement

The last calibration parameter that needs to be measured is the vector from the sensor origin to the GNSS antenna phase center (APC). This is required to translate the GNSS range measurements from the APC to the sensor origin where they are processed together with the IMU data. Again, this lever arm needs to be measured to better than the GNSS accuracy of a few cm, which is easily achieved with standard measuring devices, especially on a small UAV. While these best practices for integration may seem complicated, one of the main advantages of using a professionally integrated solution is that they are already taken care of for the user. Typically the only thing that a user needs to take care of is proper placement of the GNSS antenna and measurement of the Sensor to GNSS APC Lever Arm, and this is only if the payload is installed into a new UAV. Furthermore, the manufacturer of the payload also calibrates the camera and LiDAR so that the system is ready to go out of the box. Examples of professional UAV mapping and surveying payloads are given in Figure 3 and Figure 4.

4. BEST PRACTICES FOR OPERATION

Consistent, successful use of a mapping and surveying payload on a UAV is easily achieved with a few best practices. These are summarized in the following sections.

4.1 Mission Planning

4.1.1 Trajectory Planning

Planning the trajectory the UAV needs to fly to collect the proper data starts with understanding the type of project to be surveyed. These are typically categorized by area projects (such as a mine or a construction site) or linear projects (such as a road or a utility line corridors). For area trajectory planning the area needs to be divided into parallel flight lines with sufficient sidelap to ensure continuous coverage of the imaging sensor based upon its field of view. The flight lines need to be in opposing directions so that if necessary the overlapping sensor data can be used for a quality control process. For corridor mapping a minimum of two opposing flights lines should also be planned for the same reason.

The speed the UAV is flown at should be as high as possible for efficiency, while ensuring a specific endlap on the imagery is achieved (function of cycle time), a minimal imager smear is achieved (function of pixel size and shutter speed), and sufficient LiDAR point density is achieved (function of scan and repetition rate).

In addition, in a rotor UAV, an initial alignment procedure for the DG system must be flown right after take-off and right before landing. This consists of a simple forward-stop-backward-stop-forward procedure that can be automatically built in the UAV flight management system.

4.1.2 GNSS Augmentation System Planning

The DG system obtains cm level position from GNSS using GNSS augmentation. There are typically 3 types of GNSS augmentation methods available:

- Dedicated GNSS Base Station set up in the project area, such as the Trimble Smart Target base station (Figure 5)
- Virtual GNSS Reference Station using continuously operated GNSS reference stations (CORS) run as a service. An example of this is the Applanix POSPac SmartBase post-process VRS solution.
- Over the air or internet Precise Point correction services such as the Trimble Real-time Centerpoint RTX and POSPac Post-processed Centerpoint RTX solutions

Figure 5: Trimble Smart Target Base Station

When using a dedicated GNSS base station, the mission planning must include locating the receiver in the project area to ensure the maximum separation from the base to the UAV is no more than 5 - 10 km.

Furthermore, the base station must be surveyed or located over an existing control point, and then raw data must be logged from the receiver continuously while the UAV is being flown. In the case of a long corridor, multiple base stations must be set up to keep the baseline separation below the 10 km limit. When using a VRS or CORS data, mission planning must include ensuring that the reference stations are available in the region and that they are in sufficient density to achieve the required accuracy. To use a service like PP-RTX, planning involves making sure data from the DG system are logged for long enough time to ensure the position accuracy converges. This can be anywhere from 3 minute to 20 minutes depending upon geographic location.

4.1.3 Quality Control Planning

The final part of the mission planning involves establishing a few independent check points in the project area to check the final accuracy of the survey. The requirements on these points will be driven by the type of imaging payload being flown.

However the accuracy of the coordinates of these check points must be better than the expected accuracy of the map product, and they must be in the same datum. So if for example the accuracy goal of the UAV survey is a few cm, the accuracy of the check points must be at least 1 cm.

4.2 Data Processing

The first step after flying the survey mission is to run a quality check on the logged data to ensure it was collected correctly and it can be processed properly into the final product at the correct level of georeferencing accuracy.

For the DG system, this involves checking for data gaps in the IMU and GNSS data, checking the signal quality of the logged GNSS data, and then running the raw GNSS observations with the GNSS Augmentation through a QC step to get an indication of what the final position accuracy will be. These steps can be automated and can be done directly in the field as soon as the UAV has landed. If any part of the QC process fails, a decision can be made to re-fly or halt operations until the problem is resolved. Table 1 shows a sampel GNSS QC flight Statistics

Table 1: Sample GNSS QC Statistics

Statistics	Min	Max	Mean
Baseline length (km)	0.01	0.26	
Number of GPS SV	5	9	9
Number of GLONASS SV	0	5	5
Number of QZSS SV	0	0	0
Number of BEIDOU SV	0	0	0
Number of GALILEO SV	0	5	4
Total number of SV	5	19	18
PDOP	1.19	5.91	1.35
QC Solution Gaps	0.00	0.00	
Solution Type	Fixed	Float	No solution
Epoch (sec)	908.00	0.00	0.00
Percentage	100.00	0.00	0.00

5. BEST PRACTICES IN ACTION

The following sections present georeferencing accuracy assessments done on the data produced by professional UAV payloads that have been developed and deployed following best practices presented in the previous sections.

5.1 PhaseOne iXM-RS100 Camera System

In order to assess the performance of an integrated inertial/GNSS solution for aerial drone surveys, a number of data sets were collected in Louisville, Colorado, USA using the PhaseOne iXM-RS100 Camera system integrated with a Trimble APX-15-EI UAV direct georeferencing system. The same drone and camera payload were used in 4 consecutive flights that took place on June 17th, July 6th and July 14th, 2020. Table 2 lists the flight parameters as well as the camera dimensions. One of the objectives of assessing the geometric accuracy is to analyze the so-called *Ground Truthing*, which is the difference between the aerial-calculated and the land-surveyed check points. Therefore, a number of ground control points (GCPs) were established in the Louisville test field to be used as check points for accuracy assessment purposes. As shown in Figure 6, eleven ground control points were established in the test field using a robotic total station network that was tied into two of Trimble's continuously operating reference stations in Colorado. The estimated positioning accuracy of the 11 GCPs is 0.8 cm in Northing, Easting, and 1.2 cm in Elevation. Figure 7 shows the July 14th flight pattern.

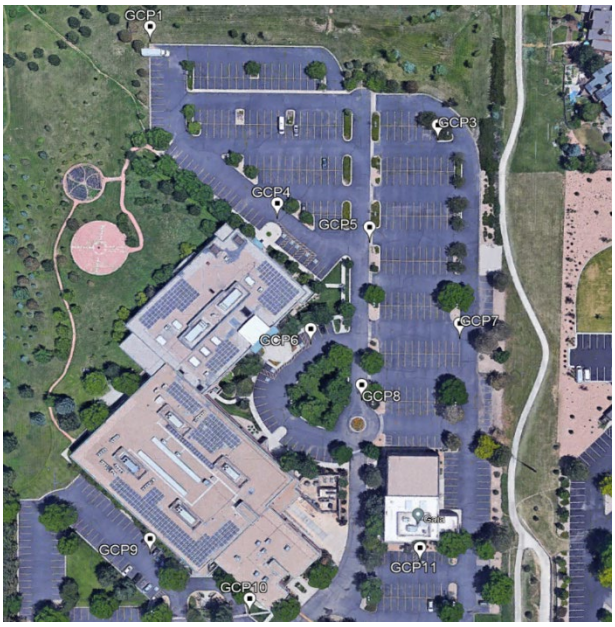

Figure 6: Ground Control Points in Louisville Test Field

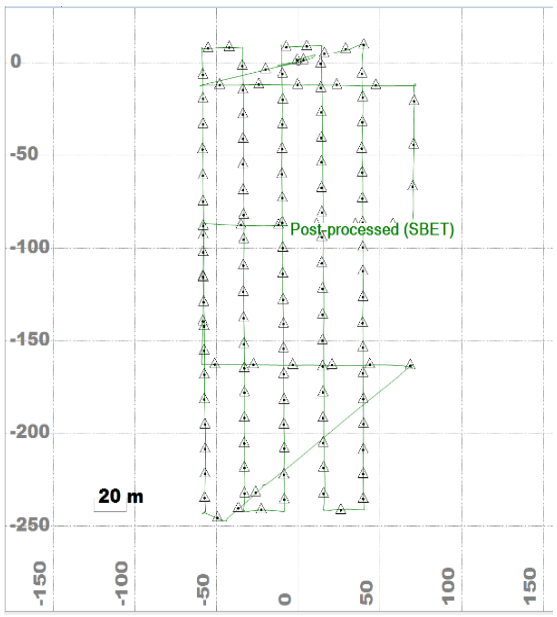

Figure 7: Louisville, CO Drone Flight Pattern

One of Trimble's continuously operating GNSS stations in Colorado was chosen as a base station for these flights due to its proximity to the test field (with a maximum baseline length of 11 Km) as shown in Figure 8. Typically, the best possible GNSS accuracy is achieved when the baseline length is within 30 Km.

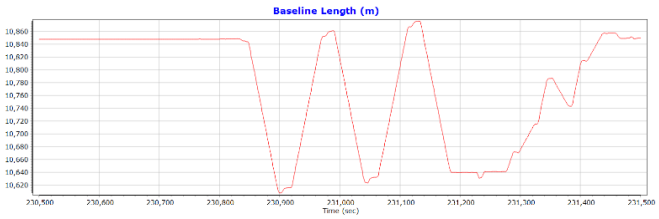

Figure 8: : Louisville Drone Flight Baseline Length (Km)

Table 2: Camera and Flight Parameters

Camera	PhaseOne iXM-RS100
Image Width	11,664 pixels
Image Length	8,750 pixels
Focal Length	35 mm
Pixel Size	3.76 µm
Flight Height	90 m AGL
GSD	1.0 cm

If the baseline length exceeds the 30 km threshold, certain errors, especially the ionospheric errors, adversely influence the positioning accuracy. In other words, the longer the baseline, the higher the positioning errors. In some cases, these errors are too high to a level that prohibits accurate ambiguity resolution.

Today's GNSS multi-frequency satellite signals including GPS, Galileo, GLONASS, and BeiDuo have the best geometry and signal to noise ratio that combined produce the highest positioning accuracy of a drone. For example, the combined PDOP for the July 14th flight does not exceed 1.5 as shown in Figure 9. PDOP is an indication of the geometric strength of satellite signals. The lower the PDOP the better the satellite geometry, the better the final positioning accuracy. The PDOP threshold for high precision surveys should not exceed 5 (Lachapelle et al, 2018). Figure 9 shows that the typical PDOP achieved nowadays is well within that threshold which results in the best possible satellite sky geometric distribution that results in the best possible positioning accuracy by GNSS.

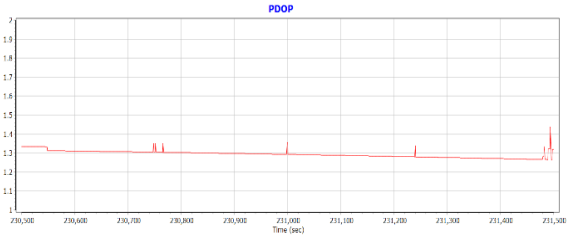

Figure 9: July 14th Drone Flight PDOP

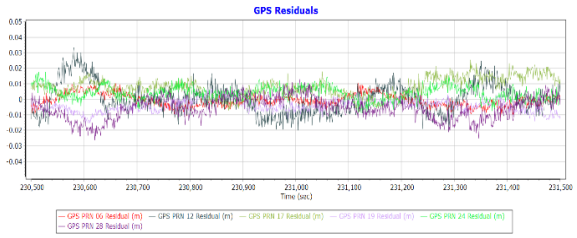

Figure 10: GPS Measurement Residuals

The GNSS signal residuals are another indication of GNSS accuracy. For example, Figure 10 shows the GPS measurement residuals which are within a maximum of 2 cm. The RMS of 0.9 cm is an indication that the absolute positioning accuracy could be at the level of 1 cm for the July 14th flight. Please note that Galileo's residuals have a 0.6 cm RMS and GLONASS residuals have a 1.2 cm RMS. Combining a number of factors leads to achieving a 1 cm level GNSS positioning accuracy. These factors are:

- Strong satellite geometry from all GNSS signals (low PDOP)
- Low satellite signal noise
- Short baseline length between a dedicated base station and the drone

Figure 11 shows the estimated positioning accuracy at the level of 1 cm in horizontal and 2 cm in vertical. Figure 12 shows that the Forward/Reverse Separation is within 5 mm.

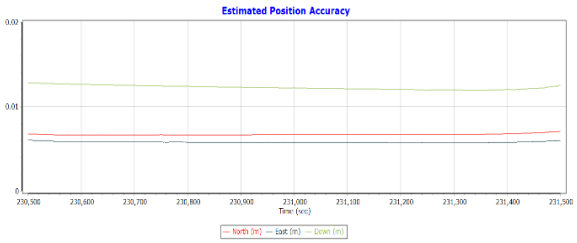

Figure 11: Estimated Positioning Accuracy

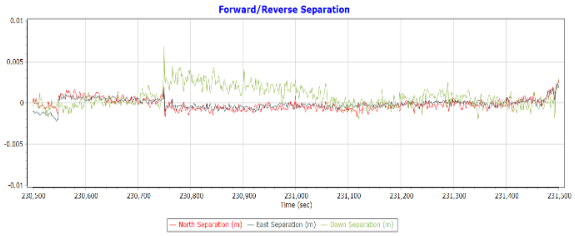

Figure 12: Forward - Reverse Separation

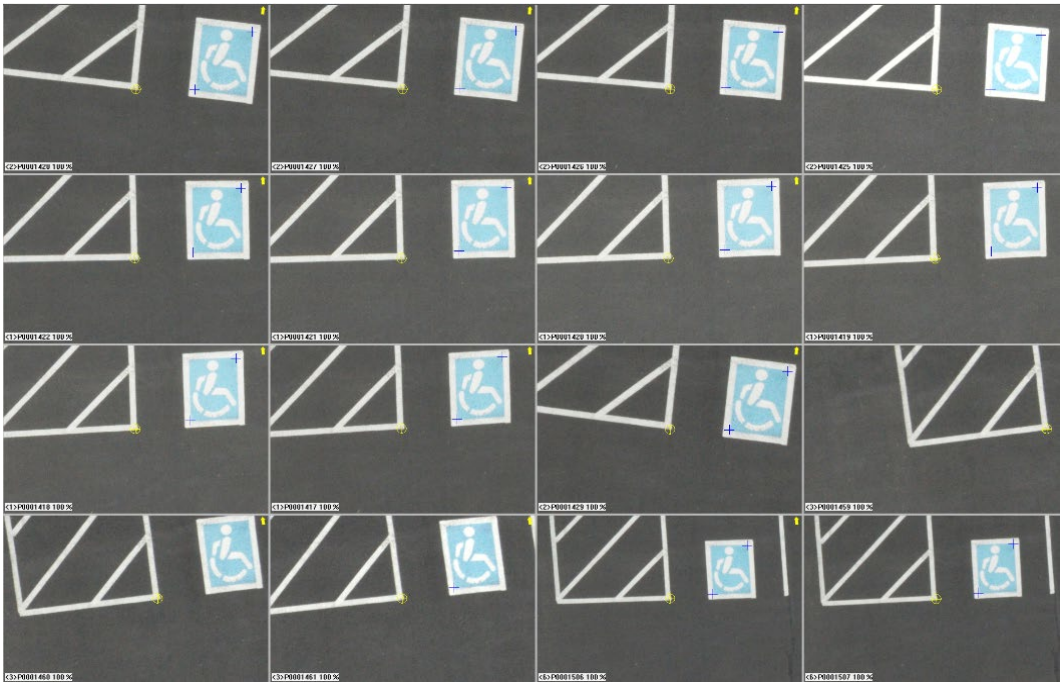

Figure 13: July 14th flight - Semi-Automated Check Point Measurement in CalQC

The drone flight pattern shown in Figure 6 allows for system calibration including camera self-calibration and boresight calibration. CalQC was used to calibrate both camera interior geometry and boresight using July 6th flight.

Then, CalQC was used to measure the checkpoints using the July 14th flight in a semi-automated mode as shown in Figure 13. CalQC measures any ground coordinates using the APX-measured Exterior Orientation parameters together with the image measurements. In other words, no ground information is used in the process and all measurements are done from the aerial data.

The coordinate difference between the land-surveyed and CalQC-measured check points are shown in Table 3 for the July 14th flight.

Table 3: July 14th CheckPoint Statistics

Check Point ID	dX (m)	dY (m)	dZ (m)
GCP1	0.02	-0.02	-0.03
GCP2	-0.02	-0.01	0.03
GCP3	-0.01	0.01	0.02
GCP4	0.00	-0.01	-0.01
GCP5	-0.01	0.01	0.02
GCP6	-0.02	0.02	0.06
GCP7	0.02	-0.03	-0.04
GCP8	-0.02	0.02	0.04
GCP9	-0.01	0.03	-0.03
GCP10	-0.02	-0.02	0.04
GCP11	0.02	-0.01	-0.04
Mean (m)	0.00	0.00	0.01
σ (m)	0.02	0.02	0.04
RMS (m)	0.02	0.02	0.04

For a 90 m flight altitude above ground resulting in a 1.0 cm GSD, the accuracy of 1-2 pixels (up to 2 cm) in horizontal and 4 pixels (up to 4 cm) in height is achievable.

5.2 GeoCue TruView 410 LiDAR System

On December 11 2019, the GeoCue TruView 410 system was flown over a test range in Huntsville, Alabama. The TruView 410 is a turn-key UAV mapping payload consisting of a Quanery M8 LiDAR integrated with two cameras and a Trimble APX-15 UAV Direct Georeferencing system. It produces high accuracy geocoded colorized point clouds, orthomosaics and final products such as volumetrics, gridded elevation data and other features such as contours and cross-sections.

The TruView 410 is part of the TruView portfolio of professional UAV LiDAR solutions offered by GeoCue. They are fully calibrated and ready to fly out of the box on a multitude of different UAV's. An example of this is shown in Figure 14 with the TruView 410 installed on a DJI M300. Figure 14 shows that the GNSS antenna has been raised above the motors to minimize shadowing and RFI interference.

Figure 14: TruView 410 on M300 UAV

The test site contained buildings and flat areas (Figur 15) and was signalized with 11 check points that were used to assess the accuracy of the final LiDAR point cloud (Figur 16).

Figur 15: Project Area

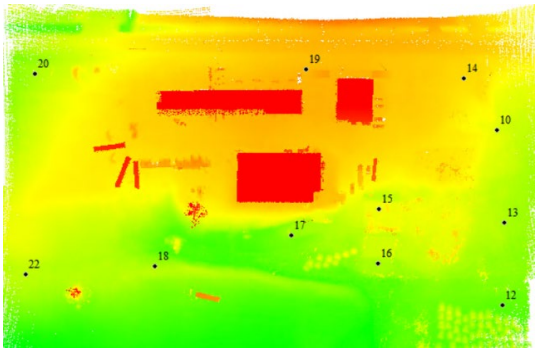

Figur 16: Check Point layout

The mission was planned following the best practices to ensure a block configuration of opposing flight lines as shown in Figure 17 with alignment procedures and a speed to ensure proper image overlap and point density (Figure 18). For this particular project extra cross strips were flown to increase the LiDAR point density to make the accuracy assessment against the checkpoints more accurate.

Figure 17: Trajectory

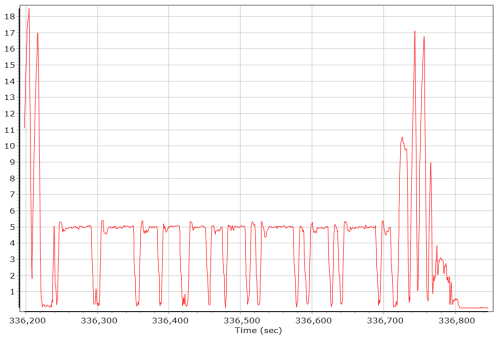

Figure 18: Speed Profile

The accuracy was assessed using two different GNSS augmentation methods: a dedicated GNSS base station and POSPac PP-RTX. The base station was set up in the project area and surveyed using the USGS OPUS service to an accuracy of less than 1 cm horizontal and 2 cm vertical.

The location of the project was in an RTX Fast region, which meant the duration of the mission of 10 minutes was sufficient to guarantee convergence to cm accuracy.

The vertical accuracy of the LiDAR point cloud was assessed by differencing the height of the 3 closest points to each check point (determined by the 3D radial position offset) with the surveyed height of the check point. The statistics for each GNSS augmentation method used are shown in Table 4.

Table 4: Height Differences vs 11 Check Points, 3 Nearest Points

	Single Base Processing			PP-RTX Processing		
	Point 1	Point 2	Point 3	Point 1	Point 2	Point 3
Mean (cm)	0.7	1.4	2.5	-0.4	-1.0	-1.4
Sigma (cm)	2.0	1.8	2.5	2.0	3.7	2.5
RMS (cm)	**2.0**	**2.2**	**2.5**	**2.0**	**3.7**	**2.7**

The results show that a professional UAV LiDAR system properly integrated with a DG system operated using best practices can easily obtain a vertical accuracy better than 4 cm RMS in the directly georeferenced point cloud, without the need for GCP's.

6. SUMMARY AND CONCLUSIONS

Accuracy assessment results have been presented for two examples of professional UAV payloads, one LiDAR + Camera based, the other Camera based, flown using best practices. The results show an absolute ground accuracy of 2 cm RMSx,y horizontal and 4 cm RMS vertical can be obtained without the use of GCP's. Using UAV's to conduct high accuracy surveys in place of ground based GNSS methods is quickly gaining acceptance due to their great increase in efficiency. While more complex to deploy than traditional techniques, a professionally integrated solution coupled with simple best practices for operation can guarantee consistent, accurate results.

REFERENCES

Casella, V., K. Jacobsen, M.M.R. Mostafa, and M. Franzini, 2006. A European Project on Direct Georeferencing, Proceedings, ASPRS Annual conference, Reno, Nevada, May 1-5, 2006

Colomina, I. and P. Molina, 2014. Unmanned aerial systems for photogrammetry and remote sensing: A review. *ISPRS Journal of Photogrammetry and Remote Sensing 92 (2014) 79–97*

Fraser, C.S., (1997). Digital Camera Self Calibration, ISPRS Journal of Photogrammetry & Remote Sensing, 52(1997): 149-159.

Hutton, J. , G. Lipa, D. Baustian, J. Sulik, R.W. Bruce, 2020. High Accuracy Direct Georeferencing Of the ALTUM Multi-Spectral UAV Camera and Its Application to High Theroughput Plant Phenotyping, *Int. Arch. Photogramm. Remote Sens. Spatial Inf. Sci., XLIII-B1-2020, 451–456, https://doi.org/10.5194/isprs-archives-XLIII-B1-2020-451-2020.*

Lachapelle et al, 2018. Performance Assessment of a Low Cost Hand Held GNSS Receiver's Raw Code and Carrier Phase Data, *Proceedings, 16th World Congress of the International Association of Institutes of Navigation, Tokyo, 28 Nov - 1 Dec 2018*

Li, R., M.M.R. Mostafa, C.V. Tao, C. Toth, 2004. "Mobile Mapping – Chapter 14", Manual of Photogrammetry – Fifth Edition, ISBN 1-57083-071-1, 1168 pages.

Mian, O., Lutes, J., Lipa, G., Hutton, J. J., Gavelle, E., and Borghini, S., 2016. Accuracy Assessment of Direct Georeferencing for Photogrammetric Applications on Small

Unmanned Aerial Platforms. IAPRS, Spatial Inf. Sci., XL-3/W4, 77-83, doi:10.5194/isprs-archives-XL-3-W4-77-2016, 2016.
Mostafa, M.M.R., S. Van-Wierts, and V. Huynh, 2018. Geometric Accuracy Assessment of Unmanned Digital Cameras and LiDAR Payloads, *proceedings of AfricaGeo 2018, Johannesburg, South Africa, 17-19 September 2018.*
Mostafa, M.M.R., 2017. Accuracy Assessment of Professional Grade Unmanned Systems for High Precision Airborne Mapping. *ISPRS Archives of the Photogrammetry, Remote Sensing and Spatial Information Sciences, 2017. Presented at the UAVg 2017, Bonn, Germany, September 4th – 7th, 2017*
Mostafa, M.M.R. and K.P. Schwarz, 2001. Digital image georeferencing from a multiple camera system by GPS/INS. *ISPRS Journal of Photogrammetry & Remote Sensing 56 (2001): 1-12.*
Scherzinger, B., J. Hutton, M.M.R. Mostafa, 2007. "Enabling Technologies - Chapter 10 2nd Edition", *Digital Elevation Model Technologies and Applications – Second Edition - ISBN 1-57083-082-7, 620 pages*
Škaloud, J., M. Cramer, and K.P. Schwarz, 1996. Exterior Orientation by Direct Measurement of Position and Attitude, *International Archives of Photogrammetry and Remote Sensing, 31 (B3): 125-130.*
White, S. and M. Aslaksen, 2006. NOAA's Use of Direct Georeferencing to Support Emergency Response. *Direct Georeferencing Column, PE&RS, Vol. 72 No. 6.*

CONTACTS

Dr Mohamed M. R. Mostafa
Trimble Applanix
85 Leek Crescent
Richmond Hill, Ontario
CANADA, L4B3B3
mmostafa@applanix.com
www.applanix.com